Available online at www.sciencedirect.com

ScienceDirect

journal homepage: http://www.elsevier.com/locate/rpor

Original research article

Absolute dose verification of static intensity modulated radiation therapy (IMRT) with ion chambers of various volumes and TLD detectors

Hediye Acun-Bucht[a,*], *Ebru Tuncay*[b], *Emin Darendeliler*[c], *Gönül Kemikler*[d]

[a] *Harran University, Faculty of Medicine, Department of Biophysics, Osmanbey Campus, 63300 Sanliurfa, Turkey*
[b] *Ministry of Health, İstanbul Research and Training Hospital, Samatya, İstanbul, Turkey*
[c] *İstanbul University, Facuty of Medicine, Department of Radiation Oncology, 34390 Capa, Istanbul, Turkey*
[d] *Istanbul University, Institute of Oncology, Department of Medical Physics, 34390 Capa, Istanbul, Turkey*

ARTICLE INFO

Article history:
Received 10 October 2016
Received in revised form
12 January 2018
Accepted 8 April 2018
Available online 19 May 2018

Keywords:
IMRT
Absolute dose
TLD
Ion chamber

ABSTRACT

Aim: This study aims at examining absolute dose verification of step-and-shoot intensity modulated radiation treatment (IMRT) of prostate and brain patients by use of ion chambers of two different volumes and thermoluminescent detectors (TLD).

Background: The volume of the ion chamber (IC) is very important for absolute dose verification of IMRT plans since the IC has a volume average effect. With TLD detectors absolute dose verification can be done measuring the dose of multiple points simultaneously.

Materials and methods: Ion chambers FC65-P of volume 0.65 cc and semiflex of volume 0.125 cc as well as TLDs were used to measure the central axis absolute dose of IMRT quality assurance (QA) plans. The results were compared with doses calculated by a treatment planning system (TPS). The absolute doses of off axis points located 2 cm and 4 cm away from the isocenter were measured with TLDs.

Results: The measurements of the 0.125 cc ion chamber were found to be closer to TPS calculations compared to the 0.65 cc ion chamber, for both patient groups. For both groups the root mean square (RMS) differences between doses of the TPS and the TLD detectors are within 3.0% for the central axis and points 2 cm away from the isocenter of each axis. Larger deviations were found at the field edges, which have steep dose gradient.

Conclusions: The 0.125 cc ion chamber measures the absolute dose of the isocenter more accurately compared to the 0.65 cc chamber. TLDs have good accuracy (within 3.0%) for absolute dose measurements of in-field points.

* *Corresponding author.*
E-mail addresses: acunhediye@yahoo.com (H. Acun-Bucht), ebrukemikler@yahoo.com (E. Tuncay), darendeliler@gmail.com (E. Darendeliler), gkemikler@gmail.com (G. Kemikler).

https://doi.org/10.1016/j.rpor.2018.04.001
1507-1367/

1. Background

IMRT provides dose distribution conforming to target volumes with complex geometries, by modulating beam intensities. The use of IMRT has been very useful for optimizing radiotherapy treatment by increasing the dose to the target volume and reducing it to the surrounding healthy tissues. The conformal dose distribution is obtained by use of multileaf collimators (MLC) located in the head of the linear accelerator (linac). Contrary to conformal radiotherapy (3D-CRT), the dose intensity of each IMRT field is changed in a complex way. There are two main types of IMRT; static (or step-and-shoot) and dynamic. With the static IMRT technique, modulated beams are obtained by use of multiple subfields (segments) with different shapes and intensities, whereas in dynamic IMRT such beams are obtained by modulation of leaf velocities while the beam intensity is constant.[1] Due to the complexity of both IMRT techniques, dosimetric verification of patient-specific IMRT plans has become necessary.[2] A quality assurance process for IMRT plans is typically carried out through verification of both the absolute dose given to the reference point and the two dimensional (2D) planar isodose distributions.[2,3]

Verification of IMRT dose distribution is a relative evaluation and has to be done with suitable two dimensional dosimeters, such as 2D array matrix detectors and films. Commercial array detectors consist of ICs or diodes. The 2D array detectors have advantages such as time saving, easy setup and direct readout of results. However 2D array detectors have low spatial resolution (usually > 7 mm) and this limits their usage for initial commissioning of IMRT QA. Dosimeters with high resolution such as radiographic or radiochromic films have to be used for QA of pre commissioned IMRT.[4] Earlier studies have investigated some properties of diode and chamber arrays such as linearity, reproducibility, output factors and dose rate dependence and reported that these arrays could be used for the measurement of fluence maps in IMRT plan verification.[5,6] Both types of array dosimeters have previously been examined for use in verification of IMRT fields.[7,8] By using 2D array detectors, each non uniform field in the IMRT plan can be measured either separately or superposed.

The planar dose validation can be carried out with radiochromic EBT or radiographic Kodak XV2 and EDR 2 films. Compared to array systems, film dosimetry has the advantage of high spatial resolution but at the same time has a disadvantage in terms of time consumption. The characteristics of Kodak XV2 and EDR2 films for verification of IMRT dose distribution have previously been examined. It was concluded that both could be used.[9–11] Use of radiochromic films has increased, since they are almost tissue equivalent and do not require processing in order to acquire optical density. Gafchromic EBT, EBT2 and EBT3 have been used in order to evaluate their characteristics for patient specific QA in different cases.[12–14] However, neither Radiochromic nor Gafchromic films should be used for absolute dose verification of IMRT fields.[4]

Although absolute dose verification of the reference point can be performed with different kinds of detectors such as ICs, semiconductor detectors, TLDs, and MOSFET,[15] IC detectors are still the ones used most often for this purpose.[16] In the static IMRT technique, each intensity modulated beam consists of small subfields (beamlets or segments) in order to obtain a non-uniform dose distribution, which can have an area as large as $1 \times 1\,cm^2$. Therefore ICs with small volumes should be used especially when carrying out absolute dose measurements of small fields. Leybovich et al. reported that both 0.6 and 0.125 cc ICs can be used for absolute dose measurements for the step-and-shoot IMRT without any leakage correction.[17] TLD detectors can be used to measure the absolute doses of multiple points simultaneously and when the phantom geometry is not suitable for insertion of an IC.[4] Davidson et al. compared IMRT doses calculated by two different heterogeneity calculation algorithms of the Pinnacle TPS with doses measured with TLD-100 LiF: Mg, Ti powder. TLD powder capsules were placed into the IMRT anthropomorphic phantom in order to measure absolute dose values of contoured structures like PTV and OAR.[18] Kry et al. used TLD-100 powder capsules, inserted into an Imaging and Radiation Oncology Core (IROC)-Houston head and neck phantom, to investigate the dosimetric accuracy of the patient specific IMRT QA. They took into account the volume of the TLD capsules and compared the measured dose with the dose of the corresponding volume of interest in the TPS.[19]

2. Aim

The purpose of this study is to investigate the absolute dose verification of step-and-shoot IMRT plans for brain and prostate cases, which have different number of segments, by use of ICs of different volumes and TLD detectors.

3. Materials and methods

3.1. *IMRT treatment planning and QA plans*

Eight prostates and seven brain IMRT plans were selected for this study. Target volumes and healthy tissues for each patient group were contoured according to ICRU 62[20] by two different radiation oncologists. IMRT plans were obtained with the step-and-shoot technique from a CMS Xio TPS (Computerized Medical Systems, St. Louis, MO, USA) using an inverse planning optimization. All optimization procedures associated to doses were done with this algorithm except from the delineation of energy, gantry angles and number of beams, which were user-defined. Both IMRT groups were planned with 6 MV photon energy in a supine position. All prostate and brain cases were planned with a seven field configuration (gantry angles: 0, 45, 90, 135, 225, 270 and 315°) and five coplanar beams (gantry angles changes depending on the location, size and shape of the target volume) on a Siemens Oncor linac (Siemens Medical Solutions, Concord, CA, USA). Doses of approximately 75 Gy/25 fractions and 54 Gy/27 fractions were determined for prostate[21] and brain[22] cases respectively. With the step-and-shoot IMRT technique, subfields (segments) can have small monitor unit (MU) values depending on the inverse treatment plane optimization procedure and the algorithm of the TPS. Therefore, MU values must be checked before inverse planning. Monitor unit stability of the linac, regarding absolute dose, should be established before producing IMRT

Fig. 1 – Measurement of planar dose distribution with PTW 2D-array 729.

plans with the step-and-shoot IMRT technique. The linearity of MU to absolute dose deviates especially at low monitor unit settings.[23] Hence, subfields which have a MU value less than 5 are not included into the static IMRT plans of this study.

Thirty slices, each 1 cm thick, of RW3 (PTW, Physikalisch-Technische Werkstätten, Freiburg, Germany) solid-water phantoms were placed on top of each other to obtain a QA phantom of size $30 \times 30 \times 20$ cm. CT images of the square phantom were taken with a Schimadzu Computed Tomography (CT) (Shimadzu, Japan) device. These CT images were then exported to the CMS Xio TPS as a square RW3 solid water phantom for verification of the IMRT plans. As part of preparing a plan verification setup, the gantry angles of intensity modulated (IM) beams were set to zero degree for each IMRT plan. Each plan was loaded to the square IMRT phantom CT slices without changes made to the shape, number and MU values of the segments, whereas such were made to gantry angles and isocenter depth in order to verify the planar dose distribution and absolute doses. The isocenter point was set to a depth of 5 cm from the surface whereas the SSD (source–skin distance) was set to 95 cm for all beams.[5] Thereafter the QA plans were transferred to the Siemens Oncor linac machine for dosimetric measurement of fluence maps and the absolute doses of the points of interest.

3.2. *Measurement and evaluation of the planar dose distribution*

A 2D IC array (PTW 2D-ARRAY seven 29, Freiburg, Germany) was inserted between the RW3 solid water phantom slices in such a way that the effective measurement points of the array would be located at 5 cm depth from the surface. SSD was fixed to 95 cm. This setup (is shown in Fig. 1) was achieved by placing a 4.5 cm phantom onto the array, since the measurement points are located at 5 mm depth from the surface of the array. Measured and calculated coronal dose maps were compared by the gamma (γ)-index method with use of the PTW VeriSoft V 3.1 software. Fig. 2 demonstrates the evaluation of planar dose distribution by gamma index method for a brain patient. This method uses dose differences (DD) and distance to agreement (DTA) parameters for evaluation of 2D fluence maps with low and high dose regions and suggests a criterion such as 1 which can be smaller or larger than the calculated γ value for each comparison. Points located in measured and calculated dose areas pass the selected DD and DTA criteria if gamma < 1 and failed if gamma > 1.[24] The software calculates the percentage of the dose points which have passed the DD and DTA criteria. In this study 3 mm and 3% DD and DTA criteria were used for gamma index evaluation.[4,25] Isodoses higher than 10% of the maximum dose were evaluated.

3.3. *Absolute dose measurement with ICs*

A PTW semiflex IC of volume 0.125 cc and a Wellhöfer Scanditronix FC65-P (IBA, Sweden) IC of volume 0.65 cc were used to examine the volume effect of the IC detector on the absolute dose of the isocenter point of the IMRT plans. All absolute dose measurements were done with a field related approach, where the gantry angles of the beams were set to zero degree. ICs were placed at the isocenters of the IMRT QA plans which all were at a SAD of 100 cm distance and at 5 cm depth from the surface, whereas SSD was fixed to 95 cm. Fig. 3 presents the absolute dose measurement set of the isocenter points of the QA plans measured with ICs. The TRS-398 formalism of IAEA was used to calculate the absolute dose of the ICs readings.[26]

3.4. *Absolute dose measurement wih TLD detectors*

LiF:Mg,Cu,P (PTW, Freiburg, Germany) TLD rods of dimension $1 \times 1 \times 4$ mm were used for absolute dose measurements of isocenters and off-axis points located along x and y axes, with 2 cm intervals from the isocenter. The commercial name of those detectors is GR-200 A TLD rods and they are composed of LiF crystals which are activated by Mg, Cu and P elements. The rods are almost water equivalent and have a linear response in an extended dose scale, between 0 and 18 Gy. Doses as small as 10^{-6} Gy could be measured with this type of detectors.[27]

60 pieces of TLD rods were irradiated 10 times with a Cobalt-60 treatment machine to calibrate and gather the rods which were closest to each others in terms of read-outs. 20 rods which had a standard deviation (SD) of $\dotplus$0.8% were paired into 10 groups. One of those groups was used as a reference for calibration and was irradiated each time on a Siemens Oncor linac with 6 MV photon beams and read-out with a Fimel-LTM TLD reader before all IMRT absolute dose measurements were done. The other nine groups of rods were used to measure absolute doses of the IMRT QA plans. A matrix phantom slab with dimension of $30 \times 30 \times 1$ cm was used for TLD measurements. This phantom had holes, 4.5 mm in diameter and 1 mm deep, with a distance of 2 cm between the center of the holes, as shown in Fig. 4. TLD groups (each including 2 rods) were placed into the holes, corresponding to the isocenter point and off axis points ($\pm$2 cm and $\pm$4 cm) from the isocenter, along the x and y axes. x and y axes lie along left-right (L-R) and gun-target (G-T) direction in the linac coordinate system, respectively. The small area surrounding the 2 pieces of rods (one group) was filled up with broken old TLD rods (since they are almost water equivalent) in order to diminish the air volume inside the holes. A matrix phantom slab was inserted between the RW3 phantom slices at a depth

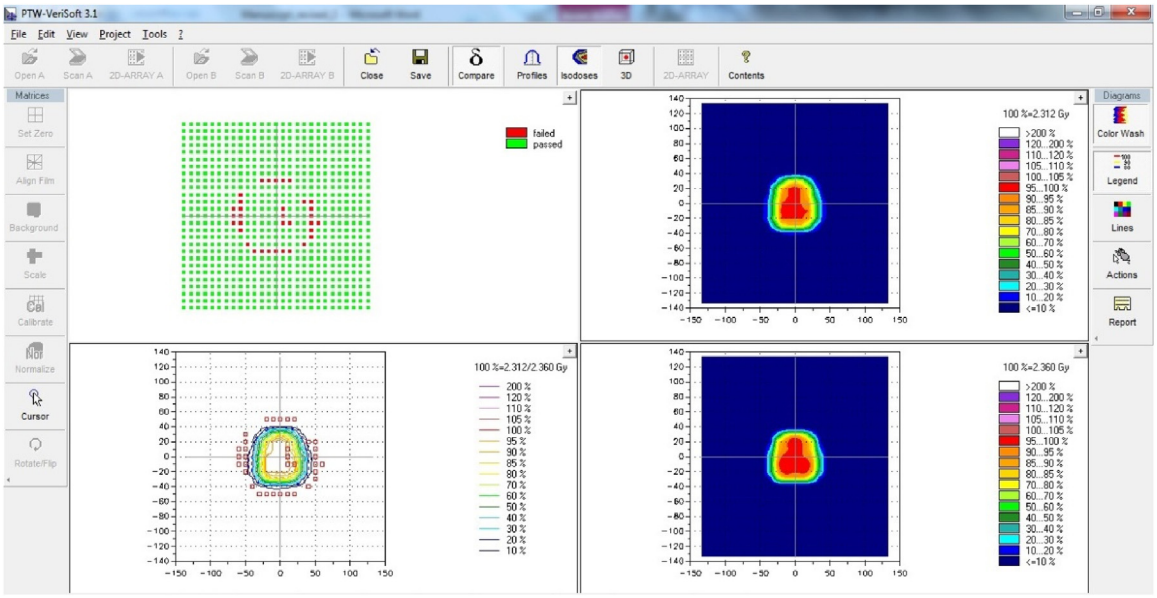

Fig. 2 – Gamma index evaluation of a brain patient's 2D dose distribution for the criteria of 3% DD and 3 mm DTA.

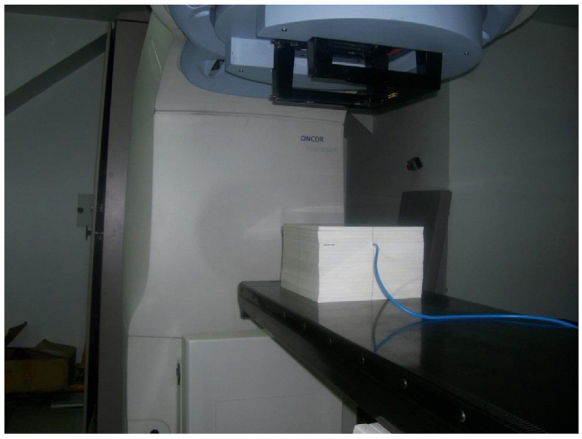

Fig. 3 – Absolute dose measurement of isocenter point with IC in a square RW3 phantom.

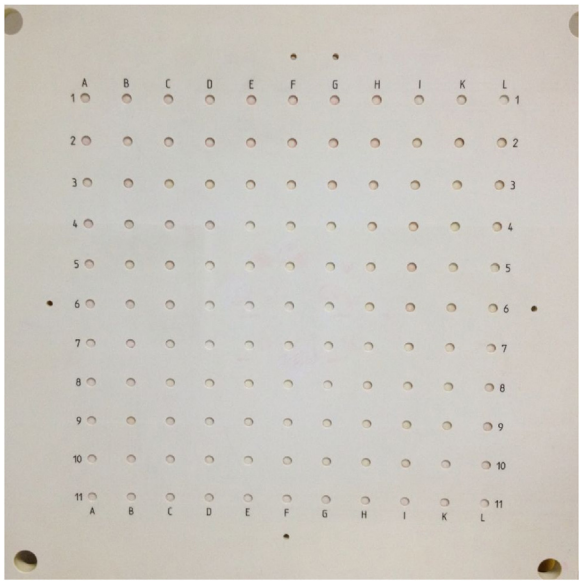

Fig. 4 – Matrix phantom slab for TLD measurements.

of 5 cm from the IMRT phantoms surface. TLD rods were at SAD 100 cm distance and SSD was 95 cm, same values as were used for the IMRT QA plan.

4. Results

The average number of segments for 8 prostate and 7 brain IMRT plans was calculated to 74.75 and 53.14 respectively. The mean values of the lowest and highest MU of the IMRT plans were 5.3–30.8 for prostate and 5.7–23.4 for brain cases. Table 1 contains the percentage of pixels passing the 3 mm and 3% (DTA/DD) criteria of the gamma evaluation method for the prostate and brain IMRT plans. More than 91% of the pixels passed the gamma evaluation for all IMRT QA plans, except for the one which had the maximum number of segments (115) in the prostate series. Fig. 5a and b compares the TPS-calculated absolute dose of the isocenter with semiflex and FC65-P ICs and with TLD detectors for prostate IMRT QA plans, respectively. The same comparisons are made in Fig. 6a and b for the brain cases. The percentage difference between calculated and measured doses is calculated according to the following equation.

$$\text{Difference}\,(\%) = \frac{\text{IC/TLD} - \text{TPS}}{\text{IC/TLD}} \times 100$$

The root mean square (RMS) value is used for evaluation of entire groups.[28] RMS is always greater than or equal to the average of the evaluated values, depending on the statistical

Table 1 – Percentage of pixels passing the 3 mm/3% gamma criteria using 2D-array for prostate and brain IMRT plans.

Prostate plans		Brain plans	
Case	Percentage of pixels passing 3 mm/3% criteria (%)	Case	Percentage of pixels passing 3 mm/3% criteria (%)
1	81.7	1	100
2	91.3	2	91.9
3	100	3	100
4	94	4	94.6
5	98.9	5	93.8
6	95.9	6	97.9
7	97.3	7	99.1
8	98.9		
Mean	94.75		96.75

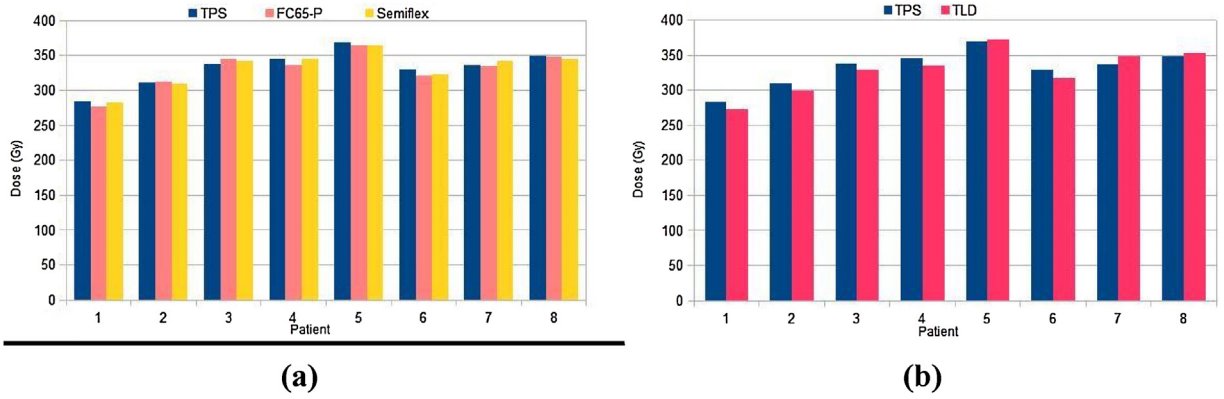

(a) (b)

Fig. 5 – Absolute dose comparison of isocenter points for prostate cases. (a) TPS versus semiflex and FC65-P ICs, (b) TPS versus TLD.

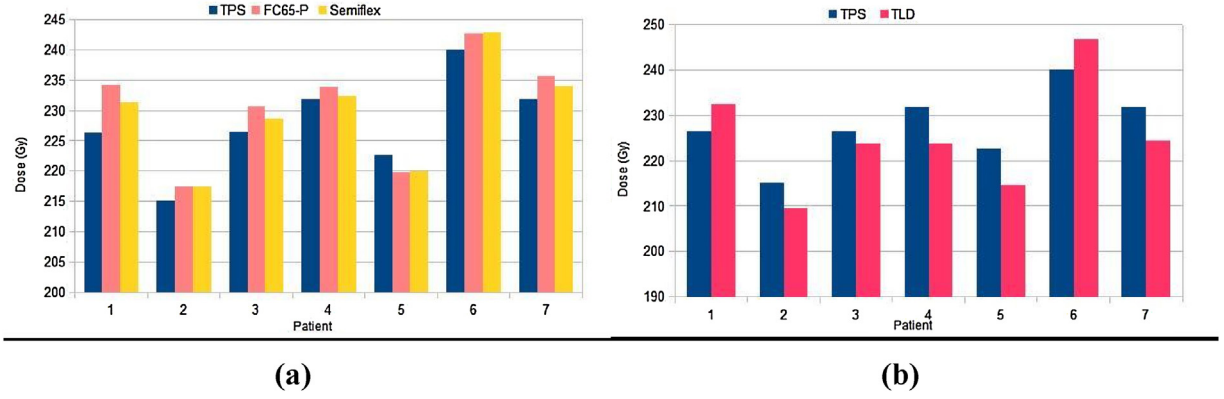

(a) (b)

Fig. 6 – Absolute dose comparison of isocenter points for brain cases. (a) TPS versus semiflex and FC65-P ICs, (b) TPS versus TLD.

deviation. Following equation, where n is the number of plans, was used for calculation of RMS.

$$\mathrm{RMS} = \sqrt{\frac{\sum \left[\frac{\mathrm{IC/TLD - TPS}}{\mathrm{IC/TLD}} \times 100\right]^2}{n}}$$

The RMS difference between isocenter doses calculated by TPS and measured with FC65-P IC are 1.56% (maximum difference is 2.56%) and 1.76% (maximum difference is 3.33%) for prostate and brain IMRT plans, respectively. The comparison of TPS and semiflex IC shows RMS differences of 1.27% (maximum difference is 2.28%) for prostate and 1.21% (maximum difference is 2.12%) for brain cases. Bigger RMS differences are observed in the TPS and TLD comparison. Those values are calculated to 2.71% (maximum difference is 3.81%) and 3.01% (maximum difference is 3.77%) for prostate and brain IMRT plans, respectively.

Tables 2 and 3 include the absolute doses calculated by TPS and measured with TLD for prostate cases and compare them with each other for off axis points laying along the left-right (LR) and gun-target (GT) directions with 2 cm intervals, respectively. The same comparisons are presented in Tables 4 and 5 for brain IMRT plans.

In cases where the points are located 2 cm from the isocenter in each direction ($x = \pm 2$ cm and $y = \pm 2$ cm), the RMS differences between doses calculated by TPS and doses

Table 2 – Comparison of the absolute doses of off-axis points, calculated by TPS and measured with TLD detectors along the x axis (LR direction) for prostate cases.

Case	+2 cm (right)			+4 cm (right)			−2 cm (left)			−4 cm (left)		
	TPS (Gy)	TLD (Gy)	Diff. (%)	TPS (Gy)	TLD (Gy)	Diff. (%)	TPS (Gy)	TLD (Gy)	Diff. (%)	TPS (Gy)	TLD (Gy)	Diff. (%)
1	288.2	279.6	−3.08	192.9	198	2.58	290.1	279.7	−3.72	226.4	216.4	−4.62
2	287.1	276.8	−3.72	150.5	144.7	−4.01	303.7	294.1	−3.26	162.4	156	−4.10
3	324.4	315.6	−2.79	197	188	−4.79	327.9	321.2	−2.09	166.1	173.5	4.27
4	332.7	320.1	−3.94	217.5	213	−2.11	325.1	315.7	−2.98	224.1	212.7	−5.36
5	340.9	349.8	2.54	234.7	222.3	−5.58	345.4	356.8	3.20	231.7	221.9	−4.42
6	353.5	346.7	−1.96	251.5	261.9	3.97	365.5	358.8	−1.87	279.9	271.3	−3.17
7	296.7	303.1	2.11	116.5	121	3.72	307.4	296.7	−3.61	123.4	128.7	4.12
8	344.1	355.8	3.29	152.5	143	−6.64	340.8	350	2.63	201.2	189.1	−6.40
RMS			3.00			4.40			2.98			4.64

Table 3 – Comparison of the absolute doses of off-axis points, calculated by TPS and measured with TLD detectors along the y axis (GT direction) for prostate cases.

Case	+2 cm (gun)			+4 cm (gun)			−2 cm (target)			−4 cm (target)		
	TPS (Gy)	TLD (Gy)	Diff. (%)	TPS (Gy)	TLD (Gy)	Diff. (%)	TPS (Gy)	TLD (Gy)	Diff. (%)	TPS (Gy)	TLD (Gy)	Diff. (%)
1	303.4	290.8	−4.33	245.7	259.5	5.32	278.1	270	−3.00	233.8	221.5	−5.55
2	297.5	288.3	−3.19	255.9	245.8	−4.11	280.8	289.5	3.01	166.5	172.3	3.37
3	337.3	326.1	−3.43	286.4	275.2	−4.07	342.6	331.9	−3.22	316.3	306.6	−3.16
4	338.9	346	2.05	311.2	321.8	3.29	320.9	312	−2.85	228.6	239.6	4.59
5	374.4	359.6	−4.12	284.4	300.8	5.45	351.9	346.4	−1.59	272.4	260.7	−4.49
6	346.4	337.6	−2.61	290.9	300.4	3.16	381.4	371.1	−2.78	251.8	245.2	−2.69
7	325.3	334.2	2.66	273.6	285.5	4.17	319.4	327.7	2.53	288.9	280.3	−3.07
8	344.9	343.2	−0.50	295.5	290.5	−1.72	351.2	335.7	−4.62	313.8	329.5	4.76
RMS			3.08			4.07			3.05			4.07

Table 4 – Comparison of the absolute doses of off-axis points, calculated by TPS and measured with TLD detectors along the x axis (LR direction) for brain cases.

Case	+2 cm (right)			+4 cm (right)			−2 cm (left)			−4 cm (left)		
	TPS (Gy)	TLD (Gy)	Diff. (%)	TPS (Gy)	TLD (Gy)	Diff. (%)	TPS (Gy)	TLD (Gy)	Diff. (%)	TPS (Gy)	TLD (Gy)	Diff. (%)
1	218.2	223.9	2.55	55.8	63	11.43	225.1	217.8	−3.35	52.2	46.3	−12.74
2	212.1	207.1	−2.41	189.5	185	−2.43	215.9	219.5	1.64	203.2	209.5	3.01
3	208.5	203.7	−2.36	39.5	35	−12.86	217.1	214.9	−1.02	45.4	41.2	−10.19
4	213.3	202.9	−5.13	125.1	120.7	−3.65	232.7	225.3	−3.28	147.3	140.4	−4.91
5	217.6	211.7	−2.79	203	197	−3.05	219.6	226.5	3.05	211.6	215.5	1.81
6	237.1	231.2	−2.55	214.5	207	−3.62	234.6	241.16	2.72	222.1	214.5	−3.54
7	217.9	225.6	3.41	210.1	217.3	3.31	238.8	232.1	−2.89	213.1	202.9	−5.03
RMS			3.16			7.05			2.69			6.97

Table 5 – Comparison of the absolute doses of off-axis points, calculated by TPS and measured with TLD detectors along the y axis (GT direction) for brain cases.

Case	+2 cm (gun)			+4 cm (gun)			−2 cm (target)			−4 cm (target)		
	TPS (Gy)	TLD (Gy)	Diff. (%)	TPS (Gy)	TLD (Gy)	Diff. (%)	TPS (Gy)	TLD (Gy)	Diff. (%)	TPS (Gy)	TLD (Gy)	Diff. (%)
1	234.5	227.5	−3.08	15.4	17	9.41	224.6	230.7	2.64	16	17.6	9.09
2	208.6	200.6	−3.99	159.8	156.1	−2.37	215.5	208.4	−3.41	183.1	190.2	3.73
3	215.1	221.3	2.80	40.5	47.8	15.27	207	212.2	2.45	46	50.1	8.18
4	230.4	226.2	−1.86	204.8	211.2	3.03	234.4	228.6	−2.54	12.7	14	9.29
5	215.7	221.6	2.66	216.8	215.4	−0.65	227.2	235.3	3.44	190.9	182.4	−4.66
6	239.8	232.27	−3.24	173.8	168.8	−2.96	237.3	227.7	−4.22	166.1	160.2	−3.68
7	230.8	238.28	3.14	227.1	236.4	3.93	230.9	238.1	3.02	226.8	219.4	−3.37
RMS			3.02			7.18			3.15			6.51

measured with TLD have similar values as RMSs for comparison of isocenter doses for both treatment cases. The discrepancies between calculated and measured doses are larger for points situated 4 cm away ($x = \pm 4$ cm and $y = \pm 4$ cm) from the isocenter, compared to those closer ($x = \pm 2$ cm and $y = \pm 2$ cm) to the center. This is the case for both brain and prostate plans. These larger deviations are found to be higher for brain cases compared to prostate cases. The reason for it is

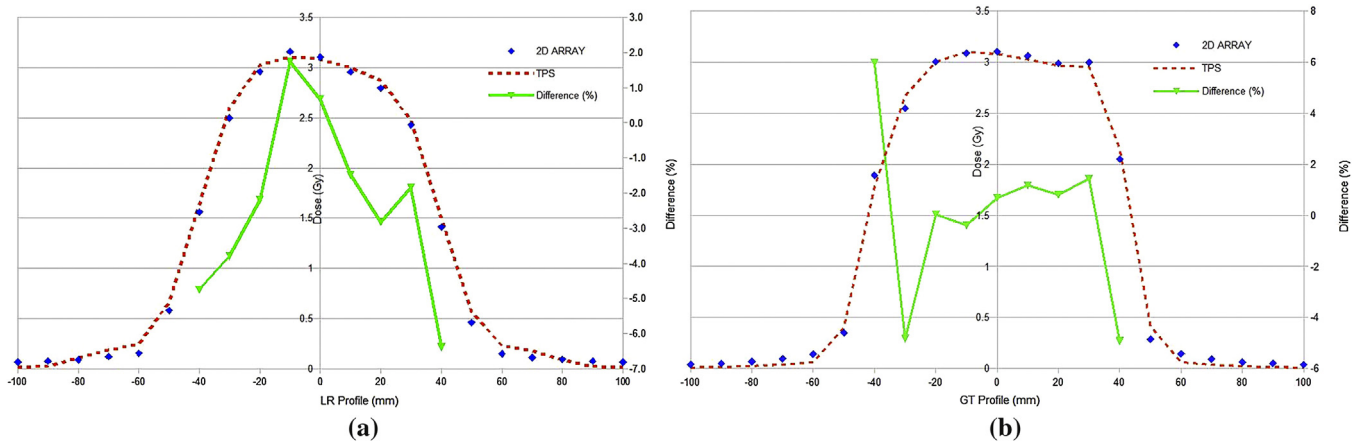

Fig. 7 – Comparison of absolute dose profiles measured by 2D array and calculated by TPS for a prostate case (a) along LR, (b) along GT directions.

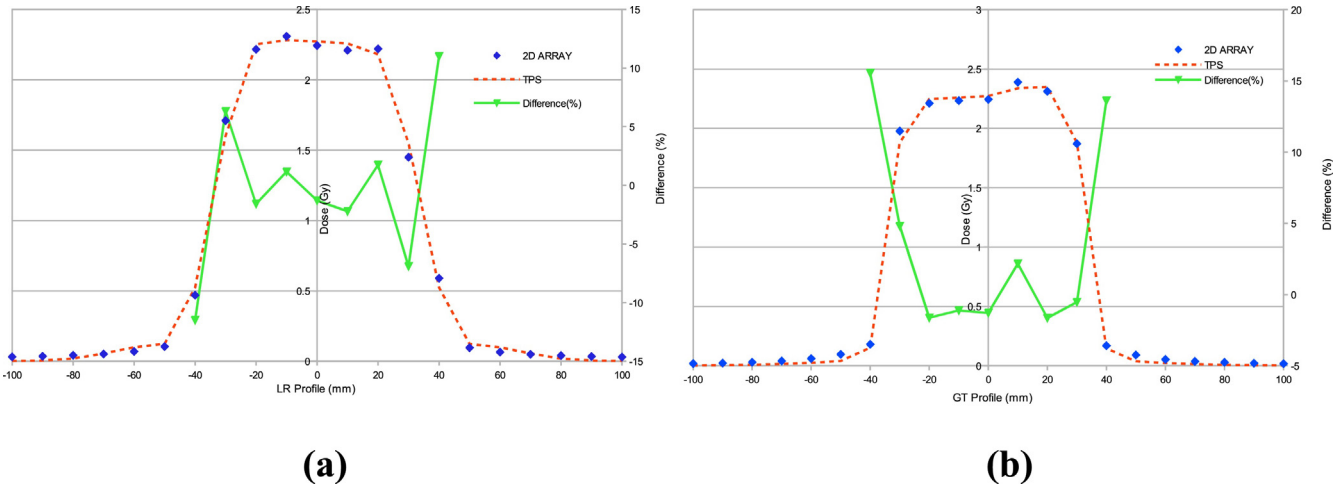

Fig. 8 – Comparison of absolute dose profiles measured by 2D array and calculated by TPS for a brain case (a) along LR, (b) along GT directions.

that the irradiation areas of the first mentioned were smaller than those obtained from the prostate IMRT plans. The absolute doses of the same off axis points were evaluated with the 2D array as well for both patient groups. Figs. 7a, b and 8a, b show the absolute dose profile taken along the LR and GT direction of a prostate and brain case, respectively. The dose difference between TPS and 2D array measurement were lower for the central point and the points located 2 cm away from the isocenter than the points placed 4 cm far from the isocenter as it is for TLD-TPS comparison for prostate and brain cases. The biggest dose differences between the TPS and the 2D array were found at the points 4 cm away from isocenter for the some brain cases which have smaller irradiation fields compared to other brain and all prostate patients.

5. Discussion

In this study, planar and absolute dose verification of 8 prostate and 7 brain IMRT plans were carried out by use of an IC 2D-array, ICs of two different volumes, as well as by use of TLD detectors. There are many studies in the literature concerning verification of IMRT dose distribution with different dosimeters. Array detectors (with ICs and diodes), Gafchromic EBT films and ICs with different volumes are frequently used for planar and absolute dose verification of the isocenter point. Mei et al. have investigated the dosimetric characteristics of a 2D IC array in terms of linearity. When it comes to planar dose verification of IMRT fields, very good agreement were found between TPS and array results for 3 mm/3% DTA and DD criteria, except from at the field edges.[29] In this study we also found larger deviations at the edges of the fields. Basran et al. studied dosimetric verification of 115 step-and-shoot IMRT patient plans, including different treatment sites, with Mapcheck diode arrays. The gamma index method was used with 3 mm/3% criteria for comparisons of planar dose distributions. The percentages of pixels passing the 3 mm/3% criteria were found to be 88% for head and neck and 95% for other treatment sites.[30] In this study, the mean percentage of pixels passing the same criteria was calculated to 94.75 for prostate cases and to 96.75% for brain cases.

Anjum et al. measured absolute doses of high and low dose regions with an NE 2571 0.6 cc IC and compared the measurements with doses calculated by TPS for head and neck and non-head and neck IMRT cases. They reported that IC results were in accordance with TPS doses, within a margin of 2.1% and 1.95%, for regions with high and low dose gradients.[13] Kinhikar et al. performed dosimetric verification of central axis and off axis points doses for 32 dynamic IMRT patients including cervix, prostate, nasopharynx and cellar tumors using 0.6 cc and 0.13 cc ICs. The mean percentage variations between the doses measured with ICs of those volumes and the doses calculated with TPS for the central axis were found to be −1.4% (with standard deviation (SD) 3.2) and −0.6% (SD 1.9). It was concluded that the IC with the smaller volume measured the dose accurately.[15] In our study RMS differences between TPS doses and doses measured with a FC65-P IC of volume 0.65 cc have been calculated to 1.56% and 1.76% for prostate and brain cases, respectively. The same comparison has RMS differences of 1.27% and 1.21% for a semiflex IC of volume 0.125 cc. A better accordance was thus observed between TPS and the smaller 0.125 cc IC compared to the larger 0.65 cc IC. The ICs are averaging the dose over the volume and this causes deviations between doses calculated by TPS and doses measured with ICs of large volumes, especially for small fields. This is an important observation to bear in mind when performing verification of central axis doses of IMRT plans, since dose distribution in IMRT could have some gradient. Therefore, the readings from ICs of larger volumes (in this case 0.65 cc) deviates more from the calculated dose compared to the smaller IC (in this case a 0.125 cc semiflex IC).

In the Khinkar et al. study, central axis and off axis (±1 cm and ±2 cm) doses of nine IMRT patients were measured with TLD chips (LiF: Mg, Ti) and the measurements were compared with TPS calculations. The mean difference was calculated to 1.8 (SD 2.9) % for TPS and TLD comparisons of central axis doses. In case of off axis doses, a variation of less than 5% was observed between doses of TPS and TLD.[15] In our study, the RMS differences between TPS and TLD for the isocenter point were calculated to 2.71% for prostate and 2.95% for brain cases. Similar RMS differences between TPS and TLD doses for the off-axis points 2 cm from the isocenter were found. The larger deviations between TPS and TLD results were found for points 4 cm further away from the isocenter (±4 cm), since those points are located at the edge of the irradiation field.

Richardson et al. performed IMRT verification of absolute doses by use of LiF TLDs (with dimensions of $1 \times 1 \times 1\,mm^3$) inserted into a spiral phantom. They found larger deviations between doses calculated by TPS and measured with TLD, as much as 6.4% at the point located in the region of the high dose gradients.[31] We also found larger deviations at points far from the central axis, which have high dose gradients. These larger deviations were higher for the brain cases compared to the prostate cases since the irradiation areas of brain IMRT plans were smaller than the prostate fields.

6. Conclusions

This study compares ICs of volumes 0.65 cc and 0.125 cc with TLD detectors in terms of absolute dose verification of step-and-shoot IMRT plans for prostate and brain cases with-different numbers of segments. The verification of 2D planar dose distribution has been carried out with a 2D ion chamber array. The mean percentage of pixels passing the 3%/3 mm criteria was calculated to a lower value for prostate cases than for brain cases. It could be concluded that this is because of the average number of segments for prostate was higher than for brain plans. 2D ion chamber arrays are very efficient for verification of planar dose distribution of IMRT fields, since they have easy setup and immediate readout of the results. In both treatment cases the readings of the 0.125 cc IC have better accordance with the doses of the central axis calculated by TPS compared to the IC of volume 0.65 cc. This is so because of volume average effect which means that the dose is averaged over the ICs active volume. This is crucial especially for point dose comparison of IMRT fields which are not homogeneous. The TLD readings are consistent with TPS calculations with deviations up to 3% for points at the central axis and up to 2 cm away from the isocenter. Larger deviations between TLD and TPS doses, up to 4%, were observed for prostate cases at the field edge and, for brain cases up to 7%, at the field edge as well as at the outside of the field. TLDs have the disadvantage of time consumption and less precision compared to ICs. On the other hand they are very efficient for multiple simultaneous point measurement.

Conflict of interest

None declared.

Financial disclosure

None declared.

REFERENCES

1. Schegel W, Bortfeld T, Grosu AL. *New technoligies in radiation oncology*. Verlag Berlin: Springer; 2006. p. 290–4.
2. Wiezorek T, Banz N, Schwedas M, et al. Dosimetric quality assurance for intensity modulated radiotherapy. *Strahlenther Onkol* 2005;**181**:468–74.
3. Ezzell GA, Galvin JM, Low D, et al. Guidance document on delivery, treatment planning, and clinical implementation of IMRT: report of the IMRT subcommittee of the AAPM radiation therapy committee. *Med Phys* 2003;**30**:2089–115.
4. Low DA, Moran JM, Dempsey JF, Dong L, Oldham M. Dosimetry tools and techniques for IMRT. *Med Phys* 2011;**38**:1313–38.
5. Spezi E, Angelini AL, Romani F, Feri A. Charecterization of a 2D ion chamber array for the verification of radiotherapy treatments. *Phys Med Biol* 2005;**50**:3361–73.
6. Létourneau D, Gulam M, Yan D, Oldham M, Wong JW. Evaluation of a 2D diode array for IMRT quality assurance. *Radiother Oncol* 2004;**70**:199–206.
7. Poppe B, Blechschmidt A, Djouguela A, et al. Two dimensional ionization chamber arrays for IMRT plan verification. *Med Phys* 2006;**33**:1005–15.
8. Buonamici FB, Compagnucci A, Marrazo L, Russo S, Bucciolini M. An intercomparison between film dosimetry and diode matrix for IMRT quality assurance. *Med Phys* 2007;**34**:1372–9.
9. Bucciolini M, Buonamici FB, Casati M. Verification of IMRT fields by film dosimetry. *Med Phys* 2004;**31**:161–70.

10. Childress NL, Salehpour M, Dong L, Bloch C, White RA, Rosen II. Dosimetric accuracy of Kodak EDR2 film for IMRT verifications. *Med Phys* 2005;**32**:539–48.
11. Zhu XR, Jursinic PA, Grimm DF, Lopez F, Rownd J, Gillin MT. Evaluation of Kodak EDR2 film for dose verification of intensity modulated radiation therapy delivered by a static multileaf collimator. *Med Phys* 2002;**29**:1687–92.
12. Zeidan OA, Stephenson SAL, Meeks SL, Wagner TH, Willoughby TR. Characterization and use of EBT radiochromic film for IMRT dose verification. *Med Phys* 2006;**33**:4064–72.
13. Anjum MN, Parker W, Ruo R, Afzal M. Evaluation criteria for film based intensity modulated radiation therapy quality assurance. *Phys Med* 2010;**26**:38–43.
14. Borca VC, Pasquino M, Russo G, et al. Dosimetric characterization and use of GAFCHROMIC EBT3 film for IMRT dose verification. *J Appl Clin Med Phys* 2013;**14**:158–71.
15. Kinhikar RA, Upreti R, Sharma S, Tambe CM, Deshpande DD. Intensity modulated radiotherapy dosimetry with ICs, TLD, MOSFET and EDR2 film. *Aust Phys Eng Sci Med* 2007;**30**:25–32.
16. Fraser D, Parker W, Seuntjens J. Characterization of cylindirical ionization chambers for patient specific IMRT QA. *J Appl Clin Med Phys* 2009;**10**:241–51.
17. Leybovich LB, Sethi A, Dogan N. Comparison of ionization chambers of various volumes for IMRT absolute dose verification. *Med Phys* 2003;**30**:119–23.
18. Davidson SE, Ibbot GS, Prado KL, Dong L. Accuracy of two heterogeneity dose calculation algorithms for IMRT in treatment plans designed using an anthropomorphic thorax phantom. *Med Phys* 2007;**34**:1850–7.
19. Kry SF, Molineu A, Kerns JR, et al. Instutional patient specific IMRT QA does not predict unacceptable plan delivery. *Int J Radiat Oncol Biol Phys* 2014;**90**:1195–201.
20. *International Comission on Radiation Units and Measurements Report, No. 50, Prescribing, Recording and Reporting Photon Beam Therapy*; 1993.
21. Pollack A, Walker G, Horwitz EM, et al. Randomized trial of hypofractionated external-beam radiotherapy for prostate cancer. *J Clin Oncol* 2013;**31**:3860–8.
22. Wagner D, Christiansen H, Wolff H, Vorwerk H. Radiotherapy of malignant gliomas: comparison of volumetric single arc technique (RapidArc), dynamic intensity-modulated technique and 3D conformal technique. *Radiother Oncol* 2009;**93**:593–6.
23. Ravikumar M, Asmary MA, Sultan RA, Ghamdi HA. Dose delivery accuracy of therapeutic photon and electron beams at low monitor unit settings. *Strahlenther Onkol* 2005;**181**:796–9.
24. Low D, Dempsey JF. Evaluation of the gamma dose distribution comparison method. *Med Phys* 2003;**30**:2455–64.
25. Rajasekaran D, Jeevanandam P, Sukumar P, Ranganathan A, Johnjothi S, Nagarajan V. A study on the correlation between plan complexity and gamma index analysis in patient specific quality assurance of volumetric modulated arc therapy. *Rep Pract Oncol Radiother* 2015;**20**:57–65.
26. International Atomic Energy Agency. Absorbed dose determination in external beam radiotherapy. In: *An International Code of Practice for Dosimetry based on standards of absorbed dose to water. Tech Rep Series No. 398*. Vienna: IAEA; 2000.
27. Bacci C, Angelo LD, Furetta C, Giancola S. Comprehensive study on LiF:Cu,Mg, P (GR-200A). *Radiat Protect Dos* 1993;**47**:215–8.
28. Seco J, Adams E, Bidmead M, Partridge M, Verhaegen F. Head-and-neck IMRT treatments with a Monte Carlo dose calculation engine. *Phys Med Biol* 2005;**50**:817–30.
29. Mei X, Bracken G, Kerr A. Evaluation of a commercial 2D ion chamber array for intensity modulated radiation therapy dose measurements. *Med Phys* 2008;**35**:3403.
30. Basran PS, Woo MK. An analysis of tolerance levels in IMRT quality assurance procedures. *Med Phys* 2008;**35**:2300–7.
31. Richardson SL, Tome WA, Orton NP, McNutt TR, Paliwal BR. IMRT delivery verification using a spiral phantom. *Med Phys* 2003;**30**:2553–8.